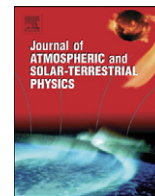




Contents lists available at ScienceDirect

Journal of Atmospheric and Solar-Terrestrial Physics

journal homepage: www.elsevier.com/locate/jastp

Systematic errors between VLBI and GPS precipitable water vapor estimations from 5-year co-located measurements

Shuanggen Jin*, O.F. Luo, J. Cho

Korea Astronomy and Space Science Institute, 61-1, Whaam-dong, Yuseong-gu, Daejeon 305-348, South Korea

ARTICLE INFO

Article history:

Received 11 September 2008

Received in revised form

8 November 2008

Accepted 30 November 2008

Available online 25 December 2008

Keywords:

Precipitable water vapor (PWV)

Systematic errors

VLBI

GPS

ABSTRACT

Space geodetic techniques (e.g., Global Positioning System, GPS and very long baseline interference, VLBI) have been widely used to determine the precipitable water vapor (PWV) for meteorology and climatology, which was verified by comparing with co-located independent technique observations. However, most of these comparisons have been conducted using only short-time spanning observations at several stations. The goal of this study is to identify and quantify the systematic errors between VLBI and GPS PWV estimates using a 5-year (2002–2007), PWV data set constructed from co-located measurements and radiosonde data as well. It has found systematic errors between VLBI and GPS PWV estimations from comparisons with long-term co-located GPS measurements. The total mean VLBI PWVs are systematically smaller than GPS estimates with 0.8–2.2 mm for all sites, but can be as much as 15–30%. The subdiurnal PWV variation magnitudes and long-term trends between VLBI and GPS are nearly similar, but the VLBI-derived PWV trends are systematically smaller than GPS estimates with about 0.1 ± 0.02 mm/year. These systematic errors in PWV estimates between VLBI and GPS are probably due to technique own problems, different used elevation angles and co-location separation.

© 2008 Elsevier Ltd. All rights reserved.

1. Introduction

The water vapor storage in the column of the atmosphere in terms of water budget is the precipitable water vapor (PWV) as a result of the balance between precipitation, evaporation and convergence of humidity (Fontaine et al., 2003). It is an important indicator of water vapor climatology and variability in the lower troposphere and related climate processes. Therefore, it is vital to measure precipitable water vapor and to understand its variability and change, but such advancements are restricted until balloon-borne radiosonde data (e.g., Bannon and Steel, 1960; Starr et al., 1965) and satellite observations from either infrared sounders or microwave radiometers (e.g., Gao et al., 2004) became available. Unfortunately, such observations are still limited in high-temporal resolution water vapor climate studies due to the poor-quality radiosonde and a lack of high spatial-temporal resolution observations as well as their costs (Gaffen et al., 1992; Elliott et al., 1995). For example, radiosondes provide vertical profile information about the meteorological variables pressure (p), temperature (T), and relative humidity (RH), but the operational cost restricts their use and also most world agencies have only

twice observations with a poor-quality per day (Westwater, 1993; Westwater et al., 2003).

The tropospheric delay is one of the major error sources for space-geodetic observations at radio wavelengths, such as Global Positioning System (GPS) and Very Long Baseline Interferometry (VLBI). Nowadays, GPS and VLBI have been widely used to determine the tropospheric zenith total delay (ZTD) (Davis et al., 1985; Gradinarsky et al., 2000; Niell et al., 2001; Jin et al., 2007) through mapping functions (Niell, 1996). The ZTD is the sum of the hydrostatic or 'dry' delay (ZHD) and non-hydrostatic or 'wet' delay (ZWD), due to the effects of dry gases and water vapor, respectively. The dry component ZHD is related to the atmospheric pressure at the surface, while the wet component ZWD can be transformed into the precipitable water vapor (Bevis et al., 1994; Duan et al., 1996; Tregoning et al., 1998; Hernandez-Pajares et al., 2001). As compared to conventional independent techniques such as satellite radiometer, ground-based microwave radiometer, and radiosondes (Westwater, 1993), it has been demonstrated that the ZTD and PWV can be retrieved using VLBI and GPS observations at the same level of accuracy as radiosondes and microwave radiometers (Elgered et al., 1997; Rocken et al., 1993; Duan et al., 1996; Emardson et al., 1998; Tregoning et al., 1998; Behrend et al., 2000). For example, Behrend et al. (2000) analyzed about 2 weeks of data during December 1996 at Madrid (Spain) and found the ZTD differences between VLBI and GPS were smaller than 1 cm. Snajdrova et al. (2005) analyzed 15 continuous

* Corresponding author. Tel.: +82 42 865 3241; fax: +82 42 861 5610.
E-mail addresses: sgjin@kasi.re.kr, sg.jin@yahoo.com (S. Jin).

days of VLBI data during the Continuous VLBI 2002 (CONT02) campaign and found that the ZTD from VLBI and GPS were in good agreement at the 3–10 mm level as well as with the Doppler Orbitography Radio positioning Integrated by Satellite (DORIS). VLBI and GPS-estimated ZTDs and PWVs are also quite good agreements with those from the European Centre for Medium-Range Weather Forecasts (ECMWF) and WVR (Heinkelmann et al., 2007). Niell et al. (2001) compared the results of a 2-week VLBI campaign in August 1995 (CONT95) at Westford (USA) with GPS, Water Vapor Radiometry (WVR) and radiosondes and found the VLBI technique was the most accurate for the determination of ZTD and PWV. These show that the VLBI and GPS can obtain a high precision and accuracy ZTD/PWV estimation for atmospheric and climatological applications. However, most of these comparisons have been done using only short time spanning observations from several weeks to several months at several stations, and almost never mention systematic errors between VLBI and GPS PWV estimates. If there exist such errors, the co-located independent measurements provide a way to calibrate another PWV data and then spread their widespread application.

In this paper, we aim to identify and quantify the systematic errors between VLBI and GPS PWV estimates using a 5-year (2002–2007), 2-hourly PWV data set constructed from ground-based co-located measurements and radiosonde data around the globe, including total mean PWV biases, diurnal sampling errors and their long-term stability. In Section 2, the details about VLBI, co-located GPS and matched radiosonde are described and their PWVs are retrieved. Section 3 presents comparison results on systematic errors in global VLBI/GPS PWV data and main summaries are given in Section 4.

2. PWV data sets

2.1. Surface meteorological data

To obtain the PWV at space geodetic sites, it needs accurate barometric pressure to calculate the zenith hydrostatic delay and temperature or relative humidity to transform the ZWD into the PWV (e.g., Bevis et al., 1994). The sensitivity of the hydrostatic delay to pressure error is $\sim 2 \text{ mm hPa}^{-1}$, so that an accuracy of $\sim 0.1 \text{ hPa}$ will insure that the error in hydrostatic delay is not significant in the measurement of the wet delay, while the sensitivity of the PWV to the surface temperature error is about $1 \text{ mm } ^\circ\text{C}^{-1}$. The current accuracies of pressure and temperature sensors at co-located VLBI and GPS sites are expected with about 0.1 hPa and $0.25 \text{ }^\circ\text{C}$, respectively. Therefore the high-accuracy PWV at VLBI and GPS sites can be obtained from these co-located pressure and temperature sensors observations with a high accuracy. In addition, as atmosphere pressure decreases exponentially with height, the height differences between the pressure sensors and the VLBI or GPS reference point are calibrated with accuracy of about 0.5 m .

2.2. VLBI PWV

The International VLBI Service for Geodesy and Astrometry (IVS) provides tropospheric products (ZTD and ZWD) of all IVS-R1 and IVS-R4 sessions since January 2002 (Schuh and Boehm 2003). All available VLBI observation data are processed by Analysis Centers (ACs) of the International VLBI Service (IVS) with three independent software packages, OCCAM, CALC/SOLVE and Steel Breeze and corresponding products (e.g., ZTD) are transferred to the IGG AC (Institute of Geodesy and Geophysics, Vienna University of Technology, Austria), for comparison and

combination. The IVS ACs are, respectively the AUS (Geoscience Australia, Australia), BKG (Bundesamt für Kartographie und Geodäsie, Germany), CNR (Istituto di Radioastronomia, Italy), DGF (Deutsches Geodätisches Forschungsinstitut, Germany), GSFC (NASA Goddard Space Flight Center, USA), IAA (Institute of Applied Astronomy, Russian), IGG (Institute of Geodesy and Geophysics, Vienna University of Technology, Austria) and MAO (Main Astronomical Observatory, National Academy of Sciences of Ukraine, Ukraine). The NASA Goddard Space Flight Center (GSFC) maintains the CALC/SOLVE and the Main Astronomical Observatory, National Academy of Sciences of Ukraine (MAO) maintains the Steel Breeze, while the OCCAM at the Institute of Applied Astronomy (IAA), Russia, are maintained and developed by different ACs (Titov et al., 2004). As individual ACs use different analysis software with different parameters and models, such as the thresholds of outlier detection, or elevation cutoff angles, it inevitably results in small but systematic differences for ZTD estimates between the solutions of the ACs. The combined ZTD product averages out those systematic differences and provides a robust and reliable basis for tropospheric parameters. For each integer hour for which at least two ACs have ZTDs, a combined ZTD is computed using a stepwise procedure. Outliers are eliminated from each time-series exceeding a $k\text{-}\sigma$ -threshold and relative weight factors are determined for each station and AC. These are used to compute the combined ZTDs as a weighted sum of the individual AC ZTDs. The detailed procedures are referred to Schuh and Boehm (2003) and Heinkelmann et al. (2007). The combined long time-series of ZTDs are determined using all geodetic VLBI sessions that are available from IVS Data Centers (<ftp://cddis.gsfc.nasa.gov/vlbi/ivsproducts/trop>). Here the 14 VLBI stations around the globe co-located with the GPS (seeing Fig. 1) are selected for the following analyses with at least 5 y observations from 2002 to 2007. The VLBI-derived ZTD time series are transformed into the PWV data with surface meteorological data.

2.3. Co-located GPS PWV

The International GNSS Service (IGS) was formally established in 1993 by the International Association of Geodesy (IAG), and began routine operations on January 1, 1994 (Beutler et al., 1999). The IGS has operated a worldwide network of permanent tracking stations with more than 350 GPS sites, and each equipped with a GPS receiver, providing raw GPS tracking data as a data format called Receiver Independent Exchange (RINEX). All available near-real-time global IGS observation data are transmitted to Global IGS Data Centers (e.g., the fourth GDC at the Korea Astronomy and Space Science Institute (KASI) (<http://gdc.kasi.re.kr>). Since 1998, the IGS regularly generates a combined tropospheric product in the form of weekly files containing the total zenith tropospheric delays (ZTD) in a 2-h time interval from the IGS tracking stations (ftp://cddis.gsfc.nasa.gov/gps/products/trop_new). The 5-year continuous combined ZTD time series are transformed into the PWV at 2-h sampling using surface meteorological data at 14 GPS sites (seeing Fig. 1) co-located with VLBI. The uncertainty of the PWV is about $0.5\text{--}1.2 \text{ mm}$.

2.4. Matched radiosonde observations

The Integrated Global Radiosonde Archive (IGRA) produced by the National Climatic Data Center (NCDC) is used in this study and is compiled from 11 datasets (Durre et al., 2006). A series of rigorous quality assurance procedures have been applied to these component datasets to create a larger and more comprehensive dataset. IGRA consists of 1–4 radiosonde observations per day at

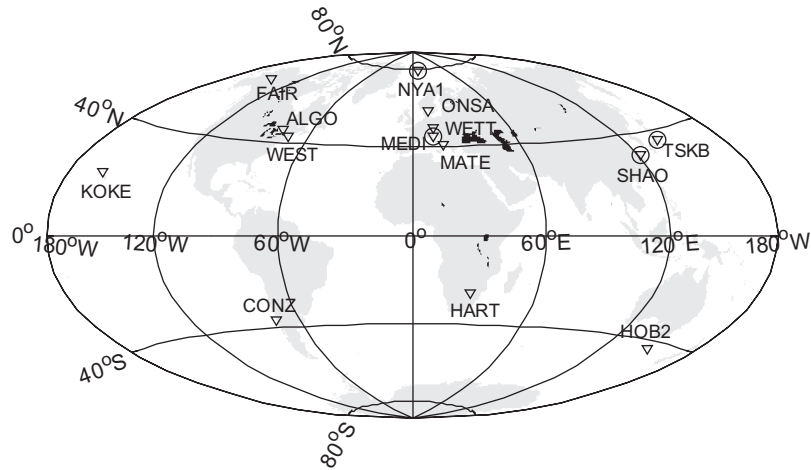


Fig. 1. Distribution of co-located VLBI (triangle), GPS (square) and radiosonde (circle) sites.

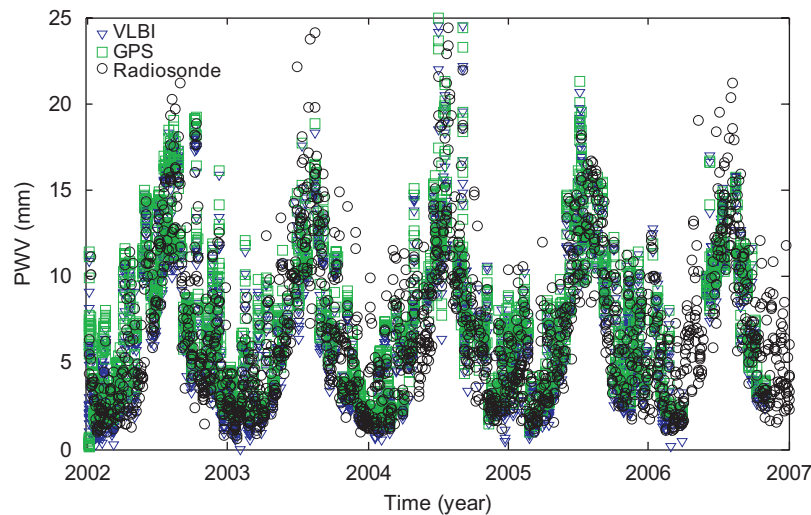


Fig. 2. PWV time series at co-located VLBI (triangle), GPS (square) and radiosonde (circle) sites in Norway (NYA1).

more than 1500 globally distributed stations from 1938 to the present. The dataset includes pressure, temperature, geopotential height, dewpoint depression, wind direction, and wind speed at standard, surface, tropopause, and significant levels (Wang and Zhang, 2008). The PWV is calculated from the IGRA data by integrating specific humidity from the surface to the top of the sounding profile (Durre et al., 2006). Global radiosondes and GPS/VLBI-PWV data from 2002 to 2007 are matched in space (both horizontally and vertically). There are a total of 4 matched pairs of stations where GPS/VLBI and radiosonde stations are located within 20 km and have elevation differences less than 20 m. The geographic distribution of matched stations is shown in Fig. 1, marked by circles.

3. Results

3.1. Total mean errors

Although VLBI-derived PWV were evaluated by comparing with other independent GPS, Water Vapor Radiometry (WVR) and radiosondes, showing good agreements (Behrend et al., 2000; Niell et al., 2001; Snajdrova et al., 2005), such demonstrations and conclusions are only from several weeks and a few stations observations. It needs to check the reliability with longer

observations at more co-located sites. Here the VLBI-derived PWV is compared with 5-year GPS PWV time series at a temporal 2-h sampling for 14 global co-located sites. For example, Fig. 2 shows PWV time series from 2002 to 2007 at co-located VLBI (triangle) and GPS (square) sites in Norway (NYA1). It can check systematic errors in PWV from long-term estimates. Fig. 3 shows histogram distributions of 5-year 2-hourly PWV differences between VLBI and GPS estimates, where the x-axis stands for the PWV difference of VLBI minus GPS and the y-axis is the number of PWV estimates. Significantly systematic errors between VLBI and GPS estimated PWV are found for all co-located sites. The VLBI-derived PWVs are systematically smaller than GPS estimates with 0–4 mm. The total mean PWV differences (VLBI minus GPS) for all available data sites are shown in Fig. 4. All of stations show that the average VLBI-derived PWV is smaller than the GPS PWV estimate with 0.8–2.2 mm and the mean difference is about 1.6 mm for all co-located sites. Also the mean differences at 13 stations are significant using *t*-test excluding nyal site.

3.2. Monthly mean errors

Mean monthly PWV values at co-located VLBI and GPS sites are calculated from whole period of data, which are used to evaluate the monthly PWV errors. Fig. 5 shows the mean monthly PWV

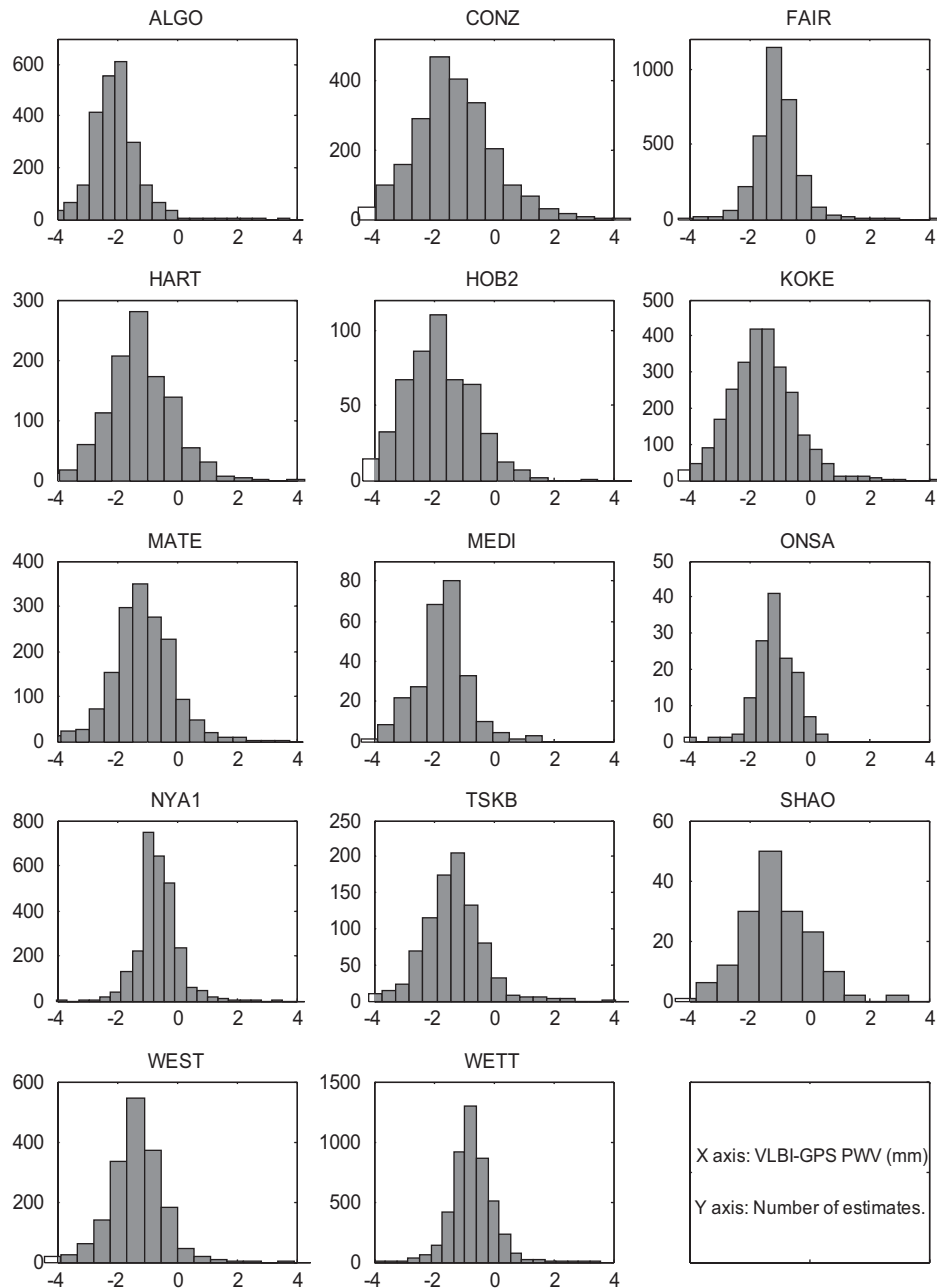


Fig. 3. Histograms of PWV differences between VLBI and GPS estimates.

(upper) and its difference (bottom) at co-located VLBI and GPS site NYA1. The absolute and relative monthly PWV differences of VLBI with respect to the GPS PWV at co-located sites are shown in Fig. 6. The left panel shows the absolute monthly PWV differences of VLBI minus GPS with 0.2–3 mm. The relative difference is defined as the monthly PWV difference of VLBI minus GPS divided by the monthly GPS PWV, expressed as percentage at the right panel of Fig. 5. Most relative differences are up to about 15–30%, indicating that the monthly VLBI-derived PWV is systematically smaller than monthly GPS-derived PWV by 15–30%.

3.3. Linear trend errors

Precipitable water vapor trend and variability in the lower troposphere is an important process of water vapor climatology

(Fontaine et al., 2003; Gradinarsky et al., 2002). Nowadays, long-term continuous GPS and VLBI observations have provided precipitable water vapor products, which have been widely applied in meteorology and climatology, including the water vapor variability and trend (Bevis et al., 1994; Elliott et al., 1995; Gendt et al., 2004; Trenberth et al., 2005; Jin et al., 2007). Here the linear trends of PWV at co-located VLBI and GPS sites are derived from 5 years of VLBI and GPS PWV, respectively (Table 1). The mean uncertainty of linear PWV trend is about 0.02 mm/year. VLBI and GPS-derived PWVs have a nearly consistent trend in Fig. 7, where the upward arrows represent the positive PWV trend and the downward arrows stand for the negative PWV trend. However, significant PWV trend differences of VLBI minus GPS are found for some co-located sites. Most of the VLBI-derived PWV trends are systematically smaller than GPS estimates with about 0.1 ± 0.02 mm/year, excluding two sites (MATE and NYA1)

(Fig. 8). The largest magnitude is up to 87% with a difference of 0.35 mm/year at CONZ site (Fig. 9).

3.4. Diurnal cycle errors

Precipitable water vapor concentrations vary with high degree of spatial and temporal variability, depending upon the season, topography and other local and regional climatic conditions (Jin et al., 2008). However, traditional observing techniques (e.g., radiosonde and radiometer) are restricted to investigate high-resolution PWV climatology and variability due to a lack of high

spatial–temporal resolution observations and the poor quality of radiosonde (e.g., Gaffen et al., 1992; Elliott et al., 1995). The long-term VLBI and GPS observations provide an important PWV set with 1–2 h’s resolution to investigate the multiscale PWV variations from sub-day to year. Here the VLBI and GPS PWV time series are analyzed using the harmonic function with periods of 1 and 0.5 day, respectively. Through the method of least squares we can determine the unknown parameters for each station using the whole 5-year PWV data set with a 1–2 h interval as well as their formal uncertainties, including amplitudes and phases of PWV variations at diurnal and semidiurnal time scales (Table 1). The mean uncertainty of diurnal and semidiurnal PWV variation amplitudes is about 0.04 mm. The diurnal and semidiurnal PWV variations between VLBI and GPS are nearly similar and most of their differences are not significant using *t*-test. However, some of subdiurnal VLBI PWV variation magnitudes are larger than GPS by 10–40%, e.g., ALGO, WEST, NYA1 and HOB2 (Fig. 10). These subdiurnal differences probably come from non-continuous VLBI observations noises.

3.5. Comparison with radiosonde

In order to further evaluate PWV errors between VLBI and GPS estimates, we compare them with co-located Radiosonde. Currently there are a total of 4 co-located GPS, VLBI and radiosonde stations. Their geographic distributions of matched stations are shown in Fig. 1. As the radiosonde has only once or twice daily observations with sparse collocated data, it is not high enough to well evaluate the diurnal cycle errors. So here the monthly PWV means from 5 years of collocated VLBI, GPS and radiosonde observations are compared in Fig. 11. The mean differences of monthly PWV from VLBI and GPS observations with respect to

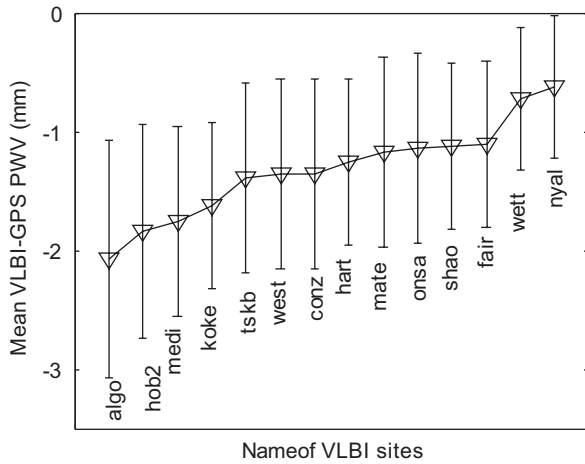


Fig. 4. Mean PWV differences of VLBI minus GPS with an uncertainty of 2σ at each co-located sites.

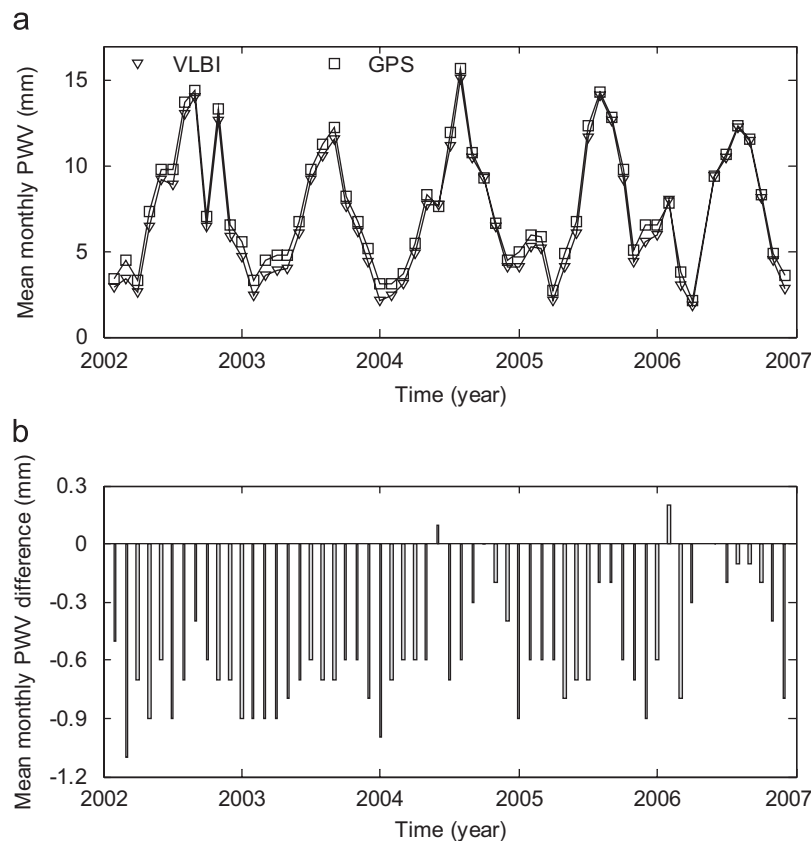


Fig. 5. Mean monthly PWV time series of VLBI (triangle) and GPS (square) at co-located site Norway (NYA1) (upper) and mean monthly PWV difference of VLBI minus GPS (bottom).

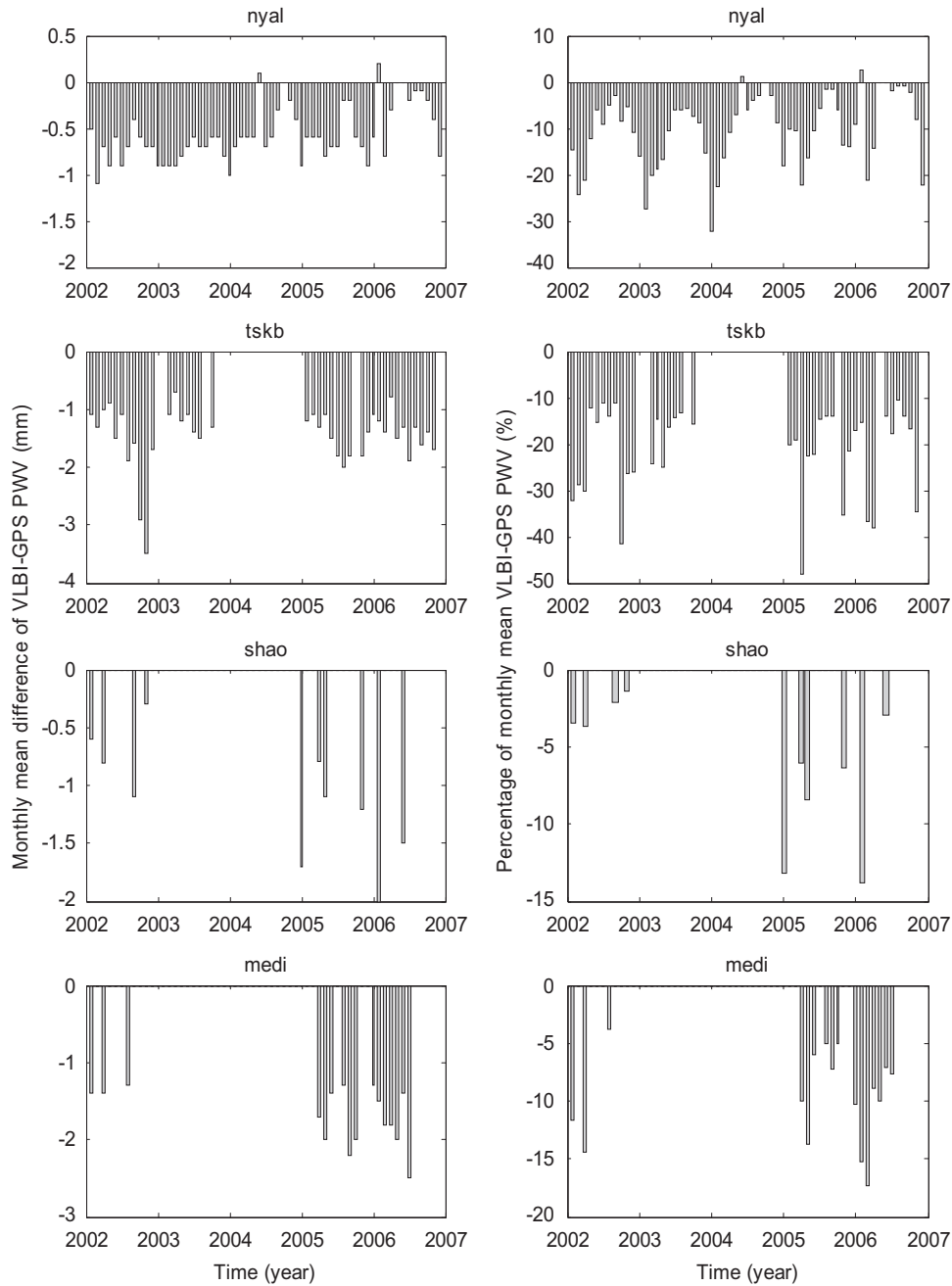


Fig. 6. Mean monthly difference (left panel) and difference percentage (right panel) of VLBI PWV with respect to the GPS PWV at co-located sites.

Table 1

Comparisons of PWV at co-located VLBI and GPS sites (Units: mm and mm/year).

VLBI station	Country	IGS acronym	Latitude	Longitude	Bias	Trend (VLBI)	Trend (GPS)	Diurnal (VLBI)	Diurnal (GPS)
Algonquin Park	Canada	ALGO	45.96	281.93	-2.07	-0.07	-0.01	0.06	0.03
Concepcion	Chile	CONZ	-36.84	286.97	-1.36	-0.40	-0.05	0.48	0.53
Gilmore Creek	USA	FAIR	64.98	212.50	-1.12	0.51	0.52	0.17	0.16
Hartebeesthoek	S. Africa	HART	-25.89	27.69	-1.26	0.85	0.98	0.74	0.74
Hobart	Australia	HOB2	-42.80	147.43	-1.84	0.36	0.42	0.69	0.83
Kokee Park	USA	KOKE	22.13	200.33	-1.62	-0.26	-0.22	0.97	1.00
Matera	Italy	MATE	40.65	16.70	-1.18	0.10	0.06	1.19	1.10
Medicina	Italy	MEDI	44.52	11.65	-1.75	0.69	0.81	1.73	1.72
Ny-Alesund	Norway	NYA1	78.93	11.87	-0.62	0.27	0.19	0.13	0.09
Onsala	Sweden	ONSA	57.40	11.93	-1.14	0.69	0.76	1.29	1.31
Shanghai	China	SHAO	31.10	121.20	-1.13	-0.33	-0.17	0.62	0.70
Tsukuba	Japan	TSKB	36.11	140.09	-1.40	2.08	2.12	0.41	0.46
Westford	USA	WEST	42.61	288.51	-1.36	0.36	0.48	0.26	0.15
Wettzell	Germany	WETT	12.89	12.89	-0.73	-0.26	-0.22	0.28	0.26

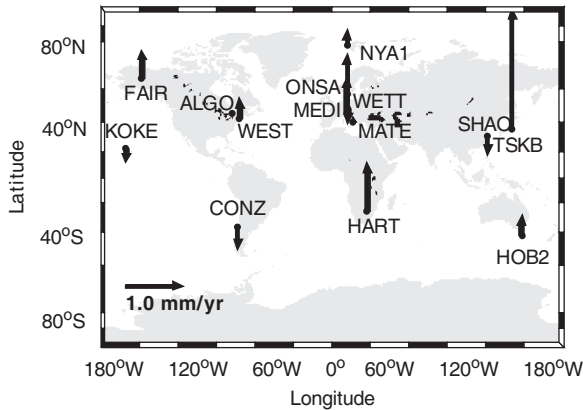


Fig. 7. Linear trend of VLBI-derived PWV.

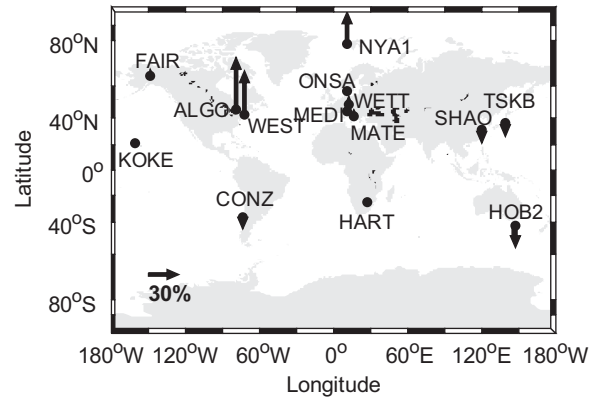


Fig. 10. Percentage of diurnal PWV magnitude difference between VLBI and GPS.

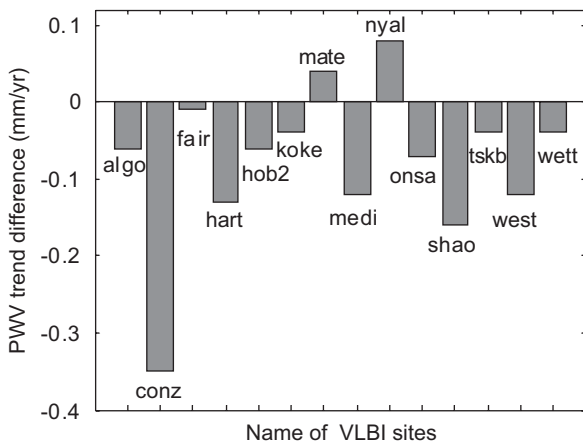


Fig. 8. Bar of linear PWV trend difference of VLBI minus GPS.

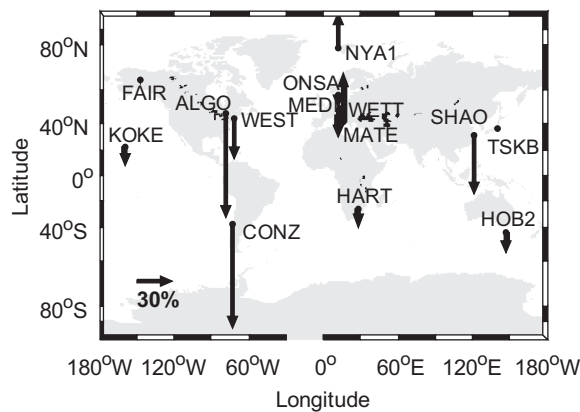


Fig. 9. Percentage of linear PWV trend difference between VLBI and GPS.

radiosonde are given in the left and right panels, respectively. It has shown a systematic error that the VLBI PWV is much smaller than the radiosonde reference value, while the GPS PWV is closer to radiosonde. However, it need to further investigate with more co-located site observations.

4. Discussions

GPS and VLBI are subject to the same errors from the atmosphere, usually referred to as the “tropospheric delay”,

including the hydrostatic or ‘dry’ delay (ZHD) and non-hydrostatic or ‘wet’ delay (ZWD). The dry component ZHD is related to the atmospheric pressure at the surface, while the wet component ZWD can be transformed into the precipitable water vapor by mapping function (Davis et al., 1985). Therefore, factors that contribute to errors in the estimate of the PWV by VLBI and GPS are the observation noise, errors in calculation of the a priori hydrostatic delay and mapping functions, possible systematic elevation-dependent changes in delay, and errors due to un-modeled effects such as azimuthal asymmetry of the atmosphere delay. These affect the estimates of PWV on different time scales. The hydrostatic mapping function generally changes on a time scale of days. The observation noise and surface pressure measurements produce errors on a scale of hours.

Here we have a series of quality checks for the GPS and VLBI ZTD estimates and other parameters required for derivation of PWV to lessen the error. For individual matched stations, we also check the GPS log files on the IGS web site (<http://igs.cb.jpl.nasa.gov/>) and VLBI log files on the IVS website (<http://ivscc.gsfc.nasa.gov/>) for any changes in ZTD that could lead to changes in PWV. The artificial ZTD changes could result from occasional changes made by individual analysis centers (ACs) in their VLBI and GPS data handling (e.g., different elevation cutoff angles) and their ZTD estimation algorithms (e.g., new mapping parameters), different constraint schemes on the analysis parameters). The possible systematic errors in the GPS PWV data are associated with the calculations of ZTD and ZHD, including elevation cutoff angles, mapping functions, satellite orbit errors, multipath and near-field scattering in the vicinity of the GPS antenna mount and a radome used for deriving ZTD. Tregoning et al. (1998) found that the PWV bias between GPS and WVR for the elevation angle from 10° to 20° is less than 1.2 mm. The 15° cut-off elevation angle was used by most of ACs, while 7°, 10° and 20° angles were used by three ACs, respectively (Gendt, 1996). The most-used high elevations will degrade effects of multipath and near-field scattering in the vicinity of the GPS antenna mount and a radome. Also, the precise orbits were used by all GPS ACs, reducing orbit error effect on PWV estimates. VLBI is not sensitive to the PWV estimates with changing elevation angle (Niell et al., 2001), and a limit of less than 0.2 mm of PWV can be set on this type of error due to the motion of the antenna, due either to deformation of the antenna itself, or to changes in electrical path length of the cables with antenna orientation (Carter et al., 1980; Herring, 1992). The mapping function causes a dry bias of less than 1 mm in the PWV estimates (Tregoning et al., 1998). However, most of VLBI and GPS ACs used the same Niell mapping function (Niell, 1996). Here the ZTDs we used are a combined solution of the ZTD values from all available GPS and VLBI ACs. Such combined ZTD solutions from all

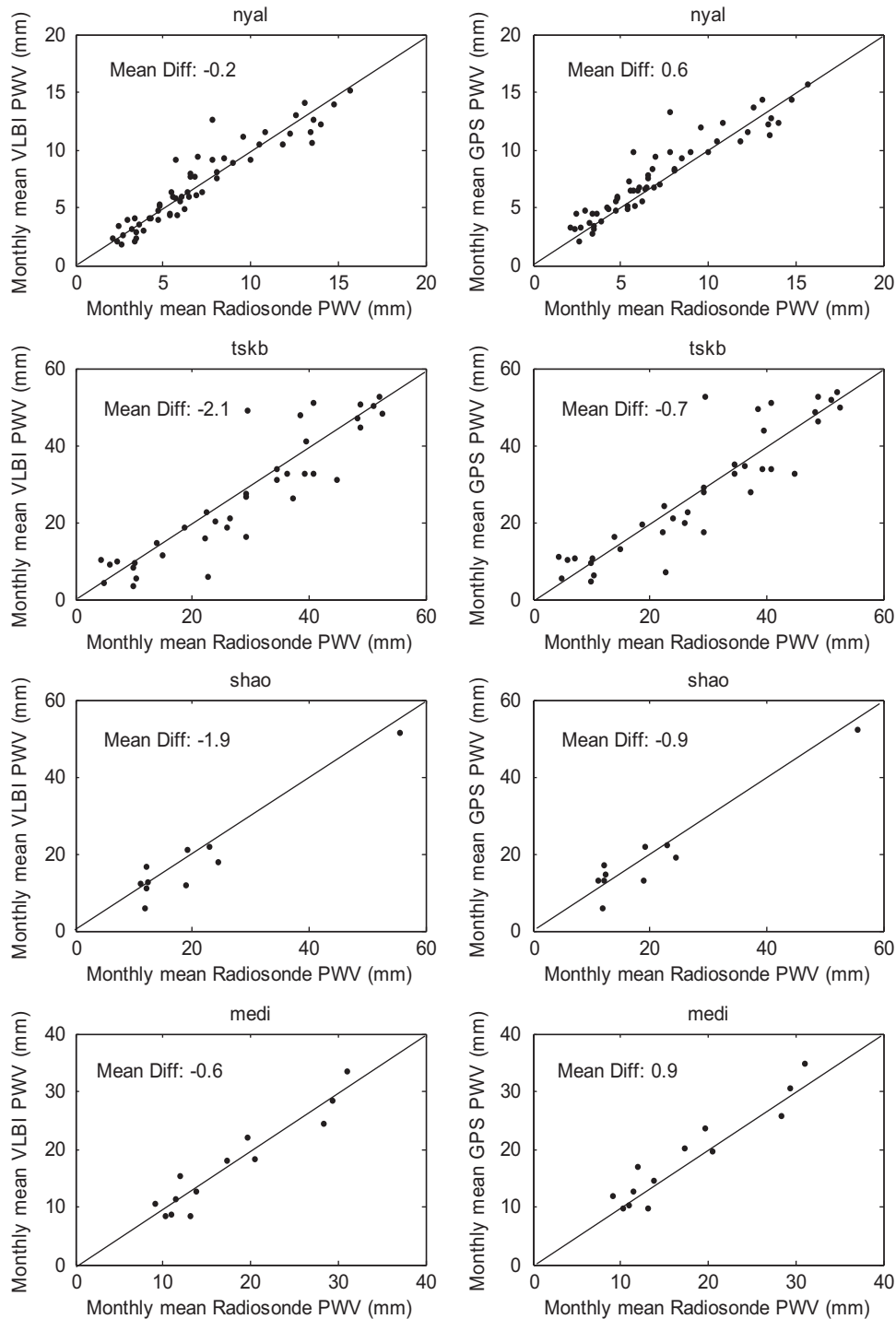


Fig. 11. Comparison of PWV from GPS and VLBI observations with radiosonde at four co-located stations (seeing Fig. 1). The mean difference is given in the legend. The GPS and VLBI station IDs are shown in the title.

GPS and VLBI ACs largely reduce the errors of ZTD solutions of GPS and VLBI, respectively. Another effect on GPS and VLBI PWV is the calculation of dry delay ZHD. However, the same formula of Saastamoinen (1973) is used to calculate the ZHD with same surface pressure data. Therefore, these factors will largely reduce the error in PWV estimates between VLBI and GPS.

Although co-located VLBI and GPS stations are within 1 km horizontally and 5 m vertically, there might still be discrepancies as a result of station separations because of variability of humidity spatially. The difference from different measurement times between the VLBI and GPS could well be random and be cancelled

out for a large number of samples. The impact of the elevation differences between VLBI and GPS stations is negligible because no significant correlations are found between PWV and elevation differences. The horizontal separation could introduce systematic differences in PWV if GPS and VLBI stations have very different humidity structures in spite of the small distance between the two stations. In order to limit this kind of problem, we check accurate locations for co-located stations and their associated terrain for any possible effects of the horizontal separation. We found that at two stations situated in the coastal regions, mean PWV differences are two or more times of their standard

deviations (representing random errors), which can be qualitatively explained by their location dissimilarities. In those regions, sharp gradients exist in the meteorological parameters including PWV.

5. Conclusion

The 5-year VLBI/GPS PWV comparisons show some systematic errors in total mean PWV, diurnal sampling, and long-term trends. The total mean VLBI PWVs are systematically smaller than GPS estimates by as much as 15–30%. The subdiurnal PWV variation magnitudes and long-term trends between VLBI and GPS are nearly similar, but some of diurnal VLBI PWV variation magnitudes are larger than GPS estimates by 10–40% and most of VLBI-derived PWV trends are systematically smaller than GPS estimates with about 0.1 ± 0.02 mm/year, about 30%. These systematic errors in PWV estimates between VLBI and GPS are mainly due to own technique problems, different used elevation angles and co-location separation. The findings clearly demonstrate the importance of independent, redundant and co-located observations for a single meteorological parameter for identification, quantification and possible correction of systematic errors. A small spatial separation for the VLBI and GPS stations could bring about a significant PWV difference. In the future, it is very important to co-locate GPS and VLBI stations as well as radiosonde. Such observations are beneficial to the PWV estimate and data quality control for co-located GPS, VLBI and radiosonde stations.

Acknowledgements

Authors thank Junhong Wang (NCAR, Boulder, CO, USA) for providing radiosonde data and IVS for providing highly precise VLBI products. This work was supported by a Grant (07KLSGC02) from Cutting-edge Urban Development-Korean Land Spatialization Research Project funded by Ministry of Land, Transport and Maritime Affairs.

References

- Bannon, J.K., Steel, L.P., 1960. Averaged water vapor contents of the air. *Geophysical Memo*, vol. 102, UK Meteorological Office M.O. 631b, 38pp.
- Behrend, D., Cucurull, L., Vila, J., Haas, R., 2000. An inter-comparison study to estimate zenith wet delays using VLBI, GPS, and NWP models. *Earth Planets Space* 52, 691–694.
- Beutler, G., Rothacher, M., Schaer, S., et al., 1999. The international GPS service (IGS): an interdisciplinary service in support of earth sciences. *Advance in Space Research* 23 (4), 631–653.
- Bevis, M., Businger, S., Chiswell, S., et al., 1994. GPS meteorology: mapping zenith wet delays onto precipitable water. *Journal of Applied Meteorology* 33, 379–386.
- Carter, W.E., Rogers, A.E., Counselmann III., C.C., Shapiro, I.I., 1980. Comparison of geodetic and radio interferometric measurements of the Haystack-Westford base line vector. *Journal of Geophysical Research* 85 (B5), 2685–2687.
- Davis, J., Herring, T., Shapiro, I., Rogers, A., Elgered, G., 1985. Geodesy by radio interferometry: effects of atmospheric modeling errors on estimates of baseline length. *Radio Sciences* 20 (6), 1593–1607.
- Duan, J., Bevis, M., Fang, P., et al., 1996. GPS meteorology: direct estimation of the absolute value of precipitable water. *Journal of Applied Meteorology* 35, 830–838.
- Durre, I., Vose, R.S., Wuertz, D.B., 2006. Overview of the integrated global radiosonde archive. *Journal of Climate* 19, 53–68.
- Elgered, G., Johansson, J., Rönnäng, B., Davis, J., 1997. Measuring regional atmospheric water vapor using the Swedish permanent GPS network. *Geophysical Research Letters* 24, 2663–2666.
- Elliott, W.P., Ross, R.J., Gaffen, D.J., 1995. Water vapor trends over North America. In: *Proceedings of Sixth Symposium on Global Change Studies*, Dallas, TX, American Meteorological Society, Preprints, pp. 185–186.
- Emardson, T., Elgered, G., Johansson, J.M., 1998. Three months of continuous monitoring of atmospheric water vapor with a network of GPS receivers. *Journal of Geophysical Research* 103, 1807–1820.
- Fontaine, B., Roucou, P., Trzaska, S., 2003. Atmospheric water cycle and moisture fluxes in the West African monsoon: mean annual cycles and relationship using NCEP/NCAR reanalysis. *Geophysical Research Letters* 30 (3), 1117.
- Gaffen, D.J., Elliott, W.P., Robock, A., 1992. Relationship between tropospheric water vapor and surface temperatures as observed by radiosondes. *Geophysical Research Letter* 19, 1839–1879.
- Gao, B.-C., Chan, P.K., Li, R.-R., 2004. A global water vapor data set obtained by merging the SSMI and MODIS data. *Geophysical Research Letters* 31, L18103.
- Gendt, G., 1996. Comparison of IGS troposphere estimations. In: Neilan, R.E., van Scoy, P.A., Zumberge, J.F. (Eds.), *Proceedings IGS 1996 Analysis Center Workshop*. IGS Central Bureau, Pasadena, pp. 151–164.
- Gendt, G., Dick, G., Reigber, C., Tomassini, M., Liu, M., Ramatschi, M., 2004. Near real time GPS water vapor monitoring for numerical weather prediction in Germany. *Journal of Meteorological Society of Japan* 82, 361–370.
- Gradinarsky, L., Haas, R., Elgered, G., Johansson, J., 2000. Wet path delay and delay gradients inferred from microwave radiometer, GPS and VLBI observations. *Earth Planets Space* 52 (10), 695–698.
- Gradinarsky, L., Johansson, J., Bouma, H., Scherneck, H.G., Elgered, G., 2002. Climate monitoring using GPS. *Physics and Chemistry of the Earth* 27 (4–5), 335–340.
- Heinkelmann, R., Boehm, J., Schuh, H., Bolotin, S., Engelhardt, G., MacMillan, D.S., Negusini, M., Skurikhina, E., Tesmer, V., Titov, O., 2007. Combination of long time-series of troposphere zenith delays observed by VLBI. *Journal of Geodesy* 81, 483–501.
- Herring, T.A., 1992. Submillimeter horizontal position determination using very long baseline interferometry. *Journal of Geophysical Research* 97, 1981–1990.
- Hernandez-Pajares, M., Juan, J., Sanz, J., et al., 2001. A new strategy for real-time integrated water vapor determination in WADGOPS networks. *Geophysical Research Letters* 28 (17), 3267–3270.
- Jin, S.G., Park, J., Cho, J., Park, P., 2007. Seasonal variability of GPS-derived zenith tropospheric delay (1994–2006) and climate implications. *Journal of Geophysical Research* 112, D09110.
- Jin, S.G., Li, Z., Cho, J., 2008. Integrated water vapor field and multi-scale variations over China from GPS measurements. *Journal of Applied Meteorology and Climatology* 47 (11), 3008–3015.
- Niell, A.E., 1996. Global mapping functions for the atmosphere delay at radio wavelengths. *Journal of Geophysical Research* 101 (B2), 3227–3246.
- Niell, A.E., Coster, A.J., Solheim, F.S., Mendes, V.B., Toor, P.C., Langley, R.B., Upham, C.A., 2001. Comparison of measurements of atmospheric wet delay by radiosonde, water vapor radiometer, GPS, and VLBI. *Journal of Atmospheric and Oceanic Technique* 18, 830–850.
- Rocken, C., Ware, R.H., Van Hove, T., Solheim, F., Alber, C., Johnson, J., Bevis, M., 1993. Sensing atmospheric water vapor with the global positioning system. *Geophysical Research Letters* 20, 2631–2634.
- Saastamoinen, J., 1973. Contribution to the theory of atmospheric refraction. *Bulletin Geodesique* 107, 13–34.
- Schuh, H., Boehm, J., 2003. Determination of tropospheric parameters within the IVS Pilot Project. *Österreichische Zeitung für Vermessung & Geoinformation (VGI)* 1/2003, 14–20.
- Snajdrova, K., Boehm, J., Willis, P., Haas, R., Schuh, H., 2005. Multi-technique comparison of tropospheric zenith delays derived during the CONT02 campaign. *Journal of Geodesy* 79 (10–11).
- Starr, V.P., Peixoto, J.P., Crisi, A.R., 1965. Hemispheric water balance for IGY. *Tellus* 17, 463–471.
- Titov, O., Tesmer, V., Boehm, J., 2004. OCCAM v.6.0 software for VLBI data analysis. In: Vandenberg, N.R., Baver, K.D. (Eds.), *IVS 2004 General Meeting Proceedings*, Ottawa, 9–11 February, pp. 267–271.
- Tregoning, P., Boers, R., O'Brien, D., 1998. Accuracy of absolute precipitable water vapor estimates from GPS observations. *Journal of Geophysical Research* 103 (28), 701–710.
- Trenberth, K.E., Fasullo, J., Smith, L., 2005. Trends and variability in column integrated atmospheric water vapor. *Climate Dynamics* 24, 741–758.
- Wang, J., Zhang, L., 2008. Systematic errors in global radiosonde precipitable water data from comparisons with ground-based GPS measurements. *Journal of Climate* 21, 2218–2238.
- Westwater, E.R., 1993. Ground-based microwave remote sensing of meteorological variables. In: Janssen, M.A. (Ed.), *Atmospheric Remote Sensing by Microwave Radiometry*. Wiley, New York, pp. 145–213.
- Westwater, E.R., Stankov, B.B., Cimini, D., Han, Y., Shaw, J.A., Lesht, B.M., Long, C.N., 2003. Radiosonde humidity soundings and microwave radiometers during Nauru99. *Journal of Atmospheric and Oceanic Technique* 20 (7), 953–971.